Hu et al. Protection and Control of Modern Power Systems (2017) 2:6
DOI 10.1186/s41601-017-0037-1

Protection and Control of Modern Power Systems

ORIGINAL RESEARCH Open Access

Optimal economic operation of isolated community microgrid incorporating temperature controlling devices

Bo Hu*, He Wang and Sen Yao

Abstract

With the increasing connection of controllable devices to isolated community microgrid, an economic operation model of isolated community microgrid based on the temperature regulation characteristics of temperature controlling devices composed of wind turbine, micro-gas turbine, energy storage battery and heat pump is proposed. With full consideration of various economic costs, including fuel cost, start-stop cost, energy storage battery depletion expense and penalty for wind curtailment, the model is solved by hybrid particle swarm optimization (HPSO) algorithm. The optimal output of the micro-sources and total operating cost of the system in the scheduling cycle are also obtained. The case study demonstrates that temperature adjustment of temperature controlling devices can adjust the power load indirectly and increase the schedulability of the isolated community microgrid, and reduce the operating cost of the microgrid.

Keywords: Isolated community microgrid, Temperature controlling devices, Economic operation, Energy storage system

1 Introduction

To solve the increasingly prominent energy crisis and environmental problems, microgrid that can accept various renewable energy sources has been developed [1–5]. However, renewable energy sources (e.g. wind energy and solar energy) in the microgrid and connection of controllable loads at the demand side have brought new challenges to microgrid scheduling and operation. The community microgrid has complicated electrical and thermal relationships due to the abundant temperature controlling devices. Therefore, adequate scheduling is the prerequisite of optimal economic operation of the community microgrid incorporating temperature controlling devices.

Optimal economic operation of microgrid is to properly allocate the output of micro-sources to increase the economic benefits of the microgrid. Many related researches have been reported. Based on the new photovoltaic output model, Reference [6] formed a probability sequence of wind-solar collaborative output through the convolution method and established a microgrid optimal economic operation model that can convert stochastic constraint into certainty constraints. The microgrid optimal economic operation model established in [7] took the impact of the electricity market into account and by optimizing the outputs of different micro-sources it reduced power fluctuation of the power lines and the total operating costs. Reference [8] put forward a multi-objective fuzzy adaptive HPSO algorithm to optimize the microgrid operation. It converted the multiple objective functions of power supply cost, environmental pollution expenses and generating cost into a single objective through the proposed algorithm. Reference [9] established a model for energy storage charge–discharge loss and incorporated it into the microgrid economic operation model to analyze its effect on the economic operation of the microgrid. In Reference [10], considering the energy storage characteristics, electric/heat load and time-of-use (TOU) power price, it proposed an economic operation model for

* Correspondence: hboy8361@163.com
State Key Laboratory of Power Transmission Equipment & System Security and New Technology, Chongqing University, Chongqing 400044, Shapingba District, China

regional connected microgrid that uses electricity-heat combined scheduling. References [11–16] considered the connection of renewable energy sources into the co-generation microgrid and the impacts of the characteristics of renewable energy power generation equipment and load randomness on optimal operation of the microgrid to optimize the outputs of different micro-sources, in order to achieve the lowest economic cost.

Based on the literature, it is found that existing researches on economic operation of microgrid mainly focus on two aspects. One studies the problems caused by volatility and intermittence of renewable energy power generation units in the microgrid and the other considers diversified energy demands in the microgrid and establishes optimal economic operation models for co-generation microgrid through independent or combined scheduling of the electric and heat systems.

However, few researches have discussed the influences of temperature controlling devices at the load side on the economic operation of microgrid. Electrical loads can be adjusted indirectly through the temperature adjustment characteristics of the temperature controlling devices, thus increasing the schedulability of the microgrid.

This paper establishes an optimal economic operation model for community microgrid incorporating temperature controlling devices with wind turbine, micro-gas turbine, energy storage battery and heat pump. With full consideration of various economic costs, including fuel cost, start-stop cost, energy storage battery depletion expenses, and penalty for wind curtailment, the model is solved by hybrid particle swarm optimization (HPSO) algorithm to achieve the optimal economic benefit. The case study validates that temperature adjustment of temperature controlling devices can reduce operating cost of the community microgrid.

2 Mathematical models for common units in the microgrid

2.1 Structure of the community microgrid

Common community microgrid generally includes renewable energy power generation equipment (e.g. wind turbine (WT) and photovoltaic (PV)) and traditional power generator sets (e.g. micro-gas turbine (MT)). Besides, it also has energy storage systems (ESS) to smooth renewable energy outputs. WT, PV and energy storage battery are controlled by the microgrid control unit. There are different types of loads connected to the microgrid. Due to large numbers of residential users in community microgrid, temperature controlling load accounts for a significant proportion. Structure of a typical community microgrid incorporating temperature controlling devices is shown in Fig. 1. The microgrid studied in this paper only has one type of renewable energy power generation equipment (i.e. WT).

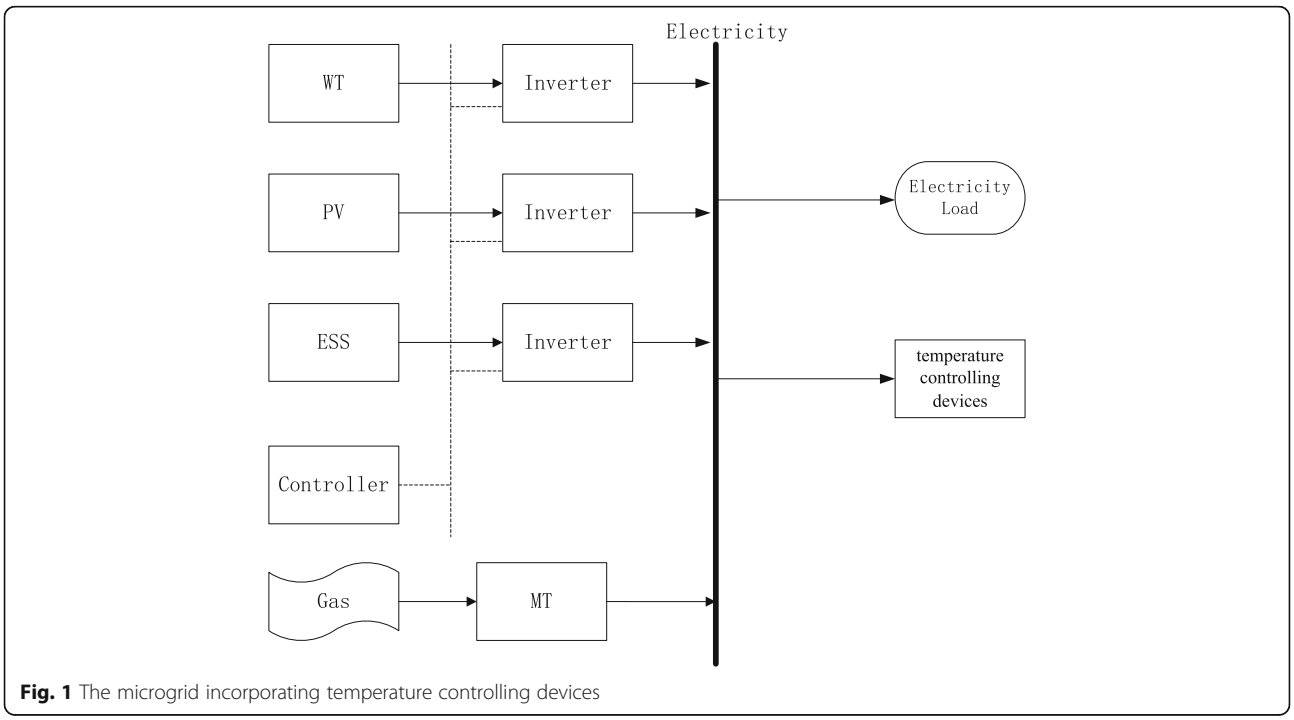

Fig. 1 The microgrid incorporating temperature controlling devices

2.2 WT output model

For distributed renewable energy generations, wind power technology is the most mature and widely used one. Due to the intermittence, randomness and instability of wind energy, WT output is influenced by meteorological factors, such as wind speed. However, the relationship between WT output and wind speed is not a simple linear one. According to many researches, WT output is related to terrain, wake effect and wind power output loss. To simplify WT output, existing studies have revealed that it is closely related to the actual wind speed of the moment. Through analyzing wind speed and WT output, it was found that WT output can be determined by the cut-in wind speed, cut-out wind speed and rated wind speed.

The relationship between WT output power and wind speed can be expressed approximately as a piecewise function [17] and a typical WT output power curve is shown in Fig. 2.

According to [17], the relationship between WT output power (P_t^w) and wind speed (v) can be approximated as:

$$P_t^w = \begin{cases} 0 & 0 \le v_t \le v_{ci} \\ P(v) & v_{ci} < v_t \le v_r \\ P_r^w & v_r < v_t < v_{co} \\ 0 & v_t \ge v_{co} \end{cases} \quad (1)$$

where v_{ci} and v_{co} are the cut-in and cut-out wind speeds, respectively. v_r is the rated wind speed and P_r^w is the rated WT output power. When the wind speed is between v_{ci} and v_r, the WT output power $P(v)$ can be approximated as an linear function of the wind speed:

$$P(v) = P_r^w \frac{(v_t - v_{ci})}{(v_r - v_{ci})} \quad (2)$$

2.3 MT output model

MT is a widely used distributed power generation equipment. It generates electricity using high-quality heat energy produced by combustion of natural gas. Compared to other distributed power generator sets that consume traditional energy sources, MT has higher energy utilization and fewer pollutant emissions. The output power of MT can be expressed as [10]:

$$P_{MT}(t) = G_{MT}(t)\eta_e q \quad (3)$$

where $P_{MT}(t)$ and $G_{MT}(t)$ are the generated output and natural gas consumption of MT during the moment t; q is the heat value of natural gas; η_e is the generating efficiency of MT during the moment t.

The fuel cost of MT during the moment t ($C_{MT}(t)$) is:

$$C_{MT}(t) = C_{\mathrm{CH4}} \cdot G_{MT}(t) \quad (4)$$

where C_{CH4} is the price of natural gas.

2.4 Charge–discharge model of the energy storage system

With increasing renewable energy sources (e.g. WT and PV) connected to the microgrid, energy storage unit which can effectively smooth renewable energy sources output and ensure reliable operation of the microgrid has become an important component. When there is renewable energy output surplus, the energy storage unit can store surplus energy to reduce wind and PV curtailment. When there is insufficient power supply, the energy storage unit can provide stable power output to the loads.

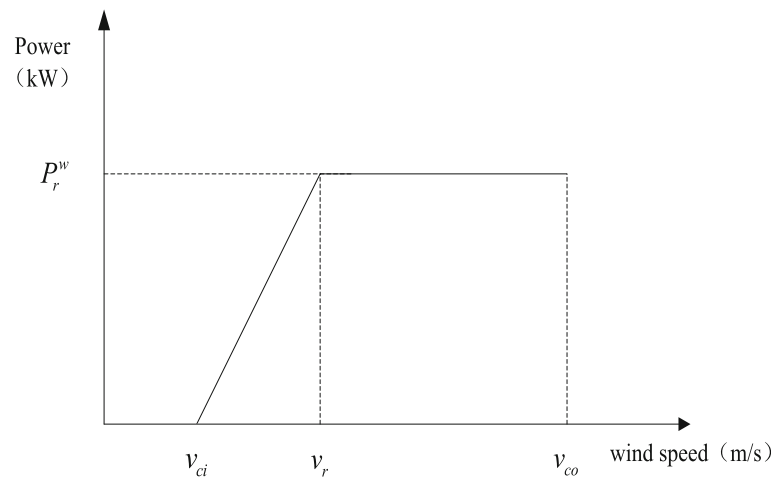

Fig. 2 Output power curve of WTG

Energy storage can generally be divided into physical energy storage and chemical energy storage. Typical physical energy storage includes pumped storage, superconducting energy storage and flywheel energy storage, whereas typical chemical energy storage includes accumulator energy storage and capacitor energy storage.

Among the different energy storages, accumulator is superior to others and has been extensively used because of its low cost, stable performance, long service life and deep charge–discharge operations. During microgrid operation, state of charge (SOC) of the energy storage system can be expressed as follows [18].

At charging stage:

$$S_{\mathrm{oc}}(t+1) = S_{\mathrm{oc}}(t) + \frac{P_t^{\mathrm{c}}\eta_{\mathrm{c}}\Delta t}{C_{bat}} \tag{5}$$

At discharging stage:

$$S_{\mathrm{oc}}(t+1) = S_{\mathrm{oc}}(t) - \frac{P_t^{\mathrm{d}}\Delta t/\eta_{\mathrm{d}}}{C_{bat}} \tag{6}$$

where $S_{oc}(t+1)$ and $S_{oc}(t)$ are the SOC of the lead-acid battery at $t+1$ and t, respectively; P_t^{c} and P_t^{d} are the charge and discharge power of the lead-acid battery at t; η_c and η_d are the charging and discharging efficiencies of the lead-acid battery; Δt is the simulation time interval (1 h in this paper); and C_{bat} is the capacity of the lead-acid battery.

3 Simulation model of typical temperature controlling devices

3.1 Equivalent model of temperature controlling devices

Community microgrid has to consider simultaneous supply of electricity and heat (temperature controlled). Typical temperature controlling devices have heat storage capacity, such as heat pump, air conditioner, water heater, etc.

In this paper, heat pump is chosen as the typical temperature controlling device. From the perspective of increasing absorption of clean energy sources, energy storage system and heat pump both store surplus energy and have similar functions. With respect to implementation, energy storage systems store surplus renewable power directly, while heat pump transforms surplus renewable power into heat energy.

Generally speaking, electricity storage has high cost and its service life can be shortened during the charge–discharge process. In contrast, heat pump has good economic benefits due to its lower investment and maintenance cost, though with higher energy consumption. Moreover, it is equipped with temperature adjustment that can adjust the total electrical load in the microgrid.

In western developed countries, temperature controlling devices like heating, ventilation and air conditioning (HVAC) system, water heater and refrigerator make great proportions of the total load. They have good energy storage characteristics and potentially can replace some energy storage devices in the microgrid [19].

According to the first principle of thermodynamics, a thermal dynamic equation (ETP) model can be established for residential energy consumption, which has been used to some extent. The equivalent electric circuit of the ETP model of a typical residential HVAC system [20] is shown in Fig. 3 and its thermal behavior is shown in Fig. 4.

In Figs. 3 and 4, C_a and C_m are the specific heat capacity of air and solids (J/℃), respectively; Q is the thermal power of the HVAC system (W); UA is the standby thermal loss coefficient (W/℃); R_1 equals to $1/UA$ and R_2 equals to $1/UA_{mass}$; T_o, T_i and T_m are the ambient temperature, indoor air temperature and the temperature of indoor solid matters (℃), respectively.

The state space description of this ETP model is:

$$\begin{cases} \dot{x} = Ax \\ y = Cx + Du \end{cases} \tag{7}$$

Where

$$\dot{x} = \begin{bmatrix} \dot{T}_i \\ \dot{T}_m \end{bmatrix} \quad x = \begin{bmatrix} T_i \\ T_m \end{bmatrix} \quad u = 1$$

$$A \begin{bmatrix} -\left(\frac{1}{R_2C_a} + \frac{1}{R_2C_a}\right) & \frac{1}{R_2C_a} \\ \frac{1}{R_2C_m} & -\frac{1}{R_2C_m} \end{bmatrix}$$

$$B = \begin{bmatrix} \frac{T_0}{R_1C_a} + \frac{Q}{C_a} \\ 0 \end{bmatrix}$$

$$C = \begin{bmatrix} 1 & 0 \\ 0 & 1 \end{bmatrix} \quad D = \begin{bmatrix} 0 \\ 0 \end{bmatrix}$$

Based on [20], Reference [21] simplified this ETP model into a first-order differential equation suitable for

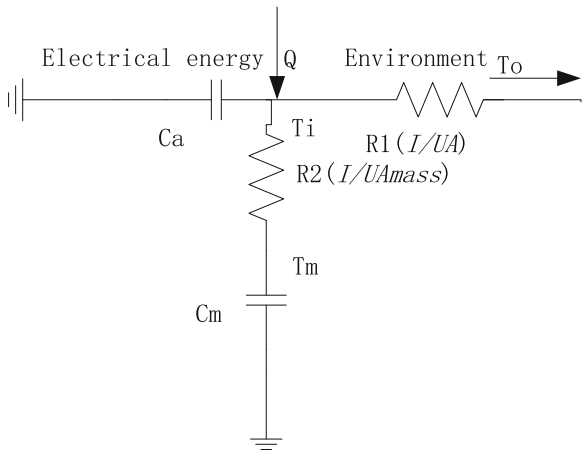

Fig. 3 Equivalent electric circuit of the ETP model of a residential HVAC system d temperature with temperature adjustment

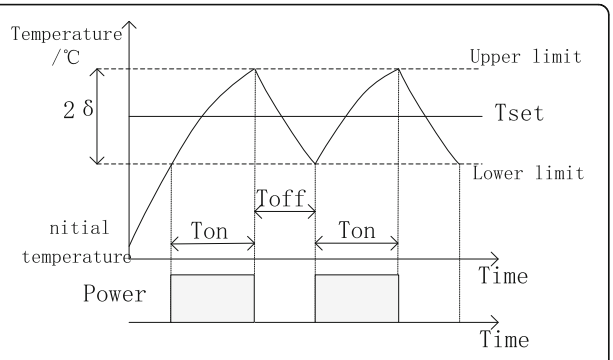

Fig. 4 Thermal behavior of a residential HVAC system

engineering analysis. For the heat pump used in this paper, when it is off,

$$T_{room}{}^{t+1} = T_{o}{}^{t+1} - \left(T_{o}{}^{t+1} - T_{room}^{t}\right) e^{-\Delta t/RC} \tag{8}$$

When it is on,

$$T_{room}{}^{t+1} = T_{o}{}^{t+1} + QR - \left(T_{o}{}^{t+1} + QR - T_{room}^{t}\right) e^{-\Delta t/RC} \tag{9}$$

where T_{room} is the indoor temperature (°C); C and R are the equivalent thermal capacitance (J/°C) and thermal resistance (°C/W), respectively; Q is the thermal power (W); T_o is the outdoor ambient temperature (°C); t is the simulation time and Δt is the simulation step size.

This ETP model keeps the main characteristics of the thermodynamic changes of the heat pump. When temperature exceeds the given upper and lower limits, the heat pump is started and begins to consume power to adjust the temperature changes, transforming electric energy into heat energy. When temperature is within the upper and lower limits, the heat pump is turned off and temperature changes naturally. This paper also employs this simplified ETP model as the simulation model of temperature controlling devices.

3.2 Operation strategy of microgrid incorporating temperature controlling devices

Community microgrid generally has strict demand of power load, but less strict requirement on temperature comfort. Therefore, temperature controlling devices in community microgrid have certain schedulability. The proposed operation strategies for community microgrid incorporating temperature controlling devices based on the temperature adjustment characteristics of temperature controlling devices is shown as follow:

① Satisfy demands for general power load in the operation period.

② Judge whether indoor temperature in this operation period is within the adjustment range. If yes, do not start the temperature controlling devices; otherwise, turn on the temperature controlling devices. These temperature controlling devices are under centralized control and indoor temperature is determined according to ambient temperature and the simulation model. Finally, power load in the community microgrid during the operation period is determined.

③ Micro-sources scheduling is adjusted according to optimized time series load power. Renewable energy power generation is used firstly, and is followed by traditional generator sets.

4 Optimal economic operation model of community microgrid incorporating temperature controlling devices

4.1 Objective function

Based on the performance features of microgrid incorporating temperature controlling devices, the objective function of the model is established, which covers several economic objective functions including MT operating cost, unit start-stop cost, depletion expense of energy storage system and penalty for wind curtailment:

$$\begin{aligned} \min F &= C_{fuel} + C_{op} + C_{wc} + C_{bat} \\ &= \sum_{t=1}^{T} \left(E_{mt}(t) \cdot f_{fuel} + f_{op}(t) + E_{wc}(t) \cdot f_{wc} \right) + C_{bat} \end{aligned} \tag{10}$$

where F is the total operation cost in the scheduling period; C_{fuel}, C_{op} and C_{wc} are the fuel cost, MT start-stop cost and wind curtailment cost in the scheduling period, respectively; C_{bat} is the depletion expense of the energy storage system; $E_{mt}(t)$ and $E_{wc}(t)$ are the fuel consumption and wind curtailment at t, respectively; f_{fuel} is the unit fuel cost and f_{wc} the unit penalty for wind curtailment; $f_{op}(t)$ is the MT start-stop cost at t. These costs can be calculated from (11–14):

$$C_{fuel} = E_{mt}(t) \cdot f_{fuel} = f_{fuel} \frac{P_t^{mt}}{\eta_e q} \Delta t \tag{11}$$

$$C_{op} = \sum_{t=1}^{T} f_{op}(t) = \sum_{t=1}^{T} \max\{0, x(t) - x(t-1)\} \cdot \left(\beta_n + \gamma_n \left(1 - e^{\left(-t'_{n,t}/\sigma_n \right)} \right) \right) \tag{12}$$

where P_t^{mt} is the generated output of MT at t; η_e is the efficiency of MT and q the heat value of natural gas; $x(t)$ is the state variable of MT: $x(t)$ =1 means turn on the MT and $x(t)$ =0 means turn off the MT; β_n, γ_n, σ_n are the

coefficients of the turn-on cost of the MT; $t'_{n,t}$ is the outage time of the MT before t.

$$C_{wc} = \sum_{t=1}^{T} E_{wc}(t) \cdot f_{wc} = \sum_{t=1}^{T} f_{wc} \cdot \left(P_t^w - P_t^{wa}\right) \Delta t \tag{13}$$

$$C_{bat} = \sum_{k=0}^{N_T} \frac{E_{in}}{N_k} \tag{14}$$

where P_t^w is the WT generated output, which can be calculated from the WT output model according to the forecasted wind speed; $P_{t^{wa}}$ is the available WT output for the microgrid; N_T is the charge–discharge cycles of the energy storage system in the scheduling period, and N_k the maximum charge–discharge cycles of the lead-acid battery [9]; E_{in} is the investment of energy storage devices in the microgrid.

4.2 Model constraints

The microgrid incorporating temperature controlling devices mainly has to meet power load balance during the operation.

① Power load balance:

$$P_{wt} + P_{mt} + P_{ess}^{dis} - P_{ess}^{ch} = P_l + P_{hp} \tag{15}$$

where P_{wt} and P_{mt} are the WT and MT output power, respectively; P_{ess}^{dis} and P_{ess}^{ch} are the discharge and charge power of the energy storage system, respectively; P_l is the general power load in the microgrid and P_{hp} the demanded power of the heat pump.

② Allowed temperature adjustment range:

$$T_{set} - \delta \le T_t \le T_{set} + \delta \tag{16}$$

where T_{set} is the set temperature and δ the temperature adjustment range after temperature comfort of users being taken into account.

③ Constraint of MT output:

$$P_{mt}^{min} \le P_{mt} \le P_{mt}^{max} \tag{17}$$

where P_{mt}^{min} is the allowed minimum output when MT is turned on and P_{mt}^{max} the allowed maximum output when MT is turned off.

④ Constraint of heat pump output

$$P_{hp}^{min} \le P_{hp} \le P_h^m \tag{18}$$

where P_{hp}^{min} and P_{hp}^{max} are the allowed minimum and maximum power when the heat pump is turned on.

⑤ Constraint of the energy storage system

Depth of charge and discharge of the energy storage system has far-reaching influence on its service life. To prevent over-charge and over-discharge of the energy storage system, the SOC constraint is:

$$Soc_{\min} \le Soc(t) \le Soc_{\max} \tag{19}$$

where $Soc_{\min}$ and $Soc_{\max}$ are the minimum and maximum SOC of the energy storage system, respectively.

Constraint of charge and discharge power of the energy storage system is:

$$P_{ess}^{ch,\min} \le P_{ess}^{ch} \le P_{ess}^{ch,\max} \tag{20}$$

$$P_{ess}^{dis,\min} \le P_{ess}^{dis} \le P_{ess}^{dis,\max} \tag{21}$$

Both large power grid and microgrid have periodic scheduling. Generally speaking, SOC of the energy storage system at the beginning and end of the scheduling period shall be the same, i.e.:

$$Soc(1) = Soc(T) = Soc_{\text{initial}} \tag{22}$$

where $Soc(1)$ and $Soc(T)$ are the SOC of the energy storage system at the beginning and end of scheduling period respectively. Soc_{initial} is the set SOC of the energy storage system at the initial scheduling period.

5 Solving method of the model

5.1 Principle of HPSO algorithm

Traditional PSO algorithm has been improved in existing researches and a hybrid particle swarm optimization (HPSO) algorithm was proposed [22]. To enrich diversity of particles, crossing and mutation operations in genetic algorithm have been introduced into qualified particles, which avoids local optimal convergence and increases the success rate of searching the optimal solution.

The crossing operation is to cross two individuals and updates individuals again to get particles out of the local optimal region and expand the search region. In this paper, updating of particle positions and speeds are:

$$\begin{cases} X_1' = X_1 \cdot rand + X_2 \cdot (1 - rand) \\ X_2' = X_2 \cdot rand + X_1 \cdot (1 - rand) \end{cases} \tag{23}$$

$$\begin{cases} V_1' = \dfrac{V_1 + V_2}{|V_1| + |V_2|} |V_1| \\ V_2' = \dfrac{V_1 + V_2}{|V_1| + |V_2|} |V_2| \end{cases} \tag{24}$$

where X_1 and X_2 are the positions of parent particles; X_1' and X_2' are the positions of offspring particles after the crossing operation; *rand* is a random number between [0,1]; V_1 and V_2 are the speeds of parent particles; V_1' and V_2' are the speeds of offspring particles after the crossing operation.

Mutation mainly decreases the convergence of particle swarm, maintains diversified feasible solutions and avoids local optimal convergence. Particles for mutation are chosen randomly according to given mutation probability.

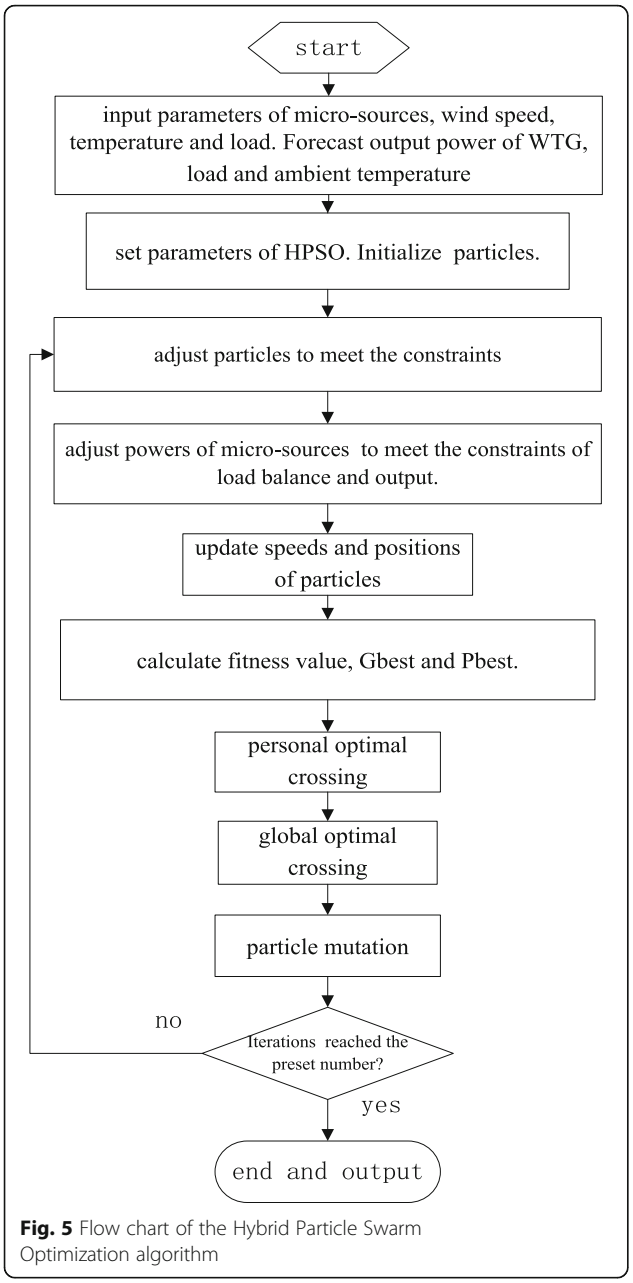

Fig. 5 Flow chart of the Hybrid Particle Swarm Optimization algorithm

5.2 Steps of the solving method based on HPSO algorithm

The established optimal economic operation model of community microgrid incorporating temperature controlling devices is solved by HPSO algorithm with the following specific steps:

Table 1 Data of the Micro turbines

Type	Power(kW)		Amount
	up	down	
MT1	20	70	1
MT2	10	50	1

Table 2 Data of the WT

Type	Power (kW)		v_{ci}	v_{co}	v_r	Amount
	up	down	(m/s)	(m/s)	(m/s)	(m/s)
WT	0	30	3	25	15	2

Step1: input parameters of the micro-sources, wind speed, temperature and load. Forecast output power of WT, load and ambient temperature.
Step2: set parameters of HPSO. Initialize the position and speed of particles, and produce the initial particle swarm.
Step3: according to the generated outputs and loads of the micro-sources, adjust the micro-source power and the energy storage system to meet the constraints of load balance and output.
Step4: calculate fitness value. The above objective function is used as the fitness value: *fitness* = *F*.
Step5: update the speeds and positions of particles. Meanwhile, the optimal personal particle and optimal global particle are updated according to the calculated fitness value.
Step6: implement the crossing and mutation operations. New particle of personal optimal crossing is gained through crossing of the personal best particles. New particle of global optimal crossing is gained through crossing of the personal best particles and global best particles. Particle mutation refers to getting new particles through mutation by themselves.
Step7: judge whether iterations have reached the preset number. If not, turn to step 3; otherwise, turn to step 8.
Step 8: end the cyclical iteration and output the global optimum and the optimal particle position. These are the optimal economic cost and outputs of the micro-sources and the energy storage system during the scheduling period.

The flow chart of this HPSO algorithm is shown in Fig. 5.

6 Case study

6.1 Brief introduction to the example

The case study is implemented based on an isolated community microgrid incorporating temperature controlling devices. This microgrid has MT, WT, energy storage device and heat pump. Parameters of these

Table 3 Parameters of the heat pumps

Type	P_{max}(kW)	P_{min}(kW)	P_r(kW)	Amount
HP	10	3	6	5

Table 4 Data of the battery

Type	Power(kW)		S_{oc}^{min} (kWh)	S_{oc}^{max} (kWh)	η_c	η_d
	$P_{ch\text{-}max}$	$P_{dis\text{-}max}$				
lead-acid battery	40	40	48	160	0.95	0.95

equipment are listed in Tables 1, 2, 3, 4, respectively. Generating efficiencies of MT1 and MT2 are 0.9 and 0.8 respectively. Heat value and price of the natural gas are set at 37 MJ/m^3 and 0.4$/m^3, respectively. β_n, γ_n and σ_n of MT1 are 5, 7 and 1, while those of MT2 are 10, 8 and 1, respectively. Penalty for unit wind curtailment in the microgrid is 2$/kW·h. Parameters related to the calculation of energy storage loss are introduced as in [9]. $SOC_{initial}$ of the energy storage device is 48kWh. In the simulation model of the temperature controlling devices, R = 0.1208 °C/W, C = 3599.3 J/W and Q = 300 W.

Forecasted results of wind power, load and ambient temperature in the coming 24 h of the scheduling period are exhibited in Figs. 6 and 7. For simplicity, their forecasting errors are neglected when solving the established model.

6.2 Example analysis

① Optimal economic operation of the microgrid without temperature adjustment

Based on the established optimal economic operation model of the microgrid, outputs of the micro-sources in the microgrid in the coming 24 h are optimized according to forecasted load, wind power and ambient temperature. The optimal power generation scheduling without temperature adjustment is shown in Fig. 8. The total system operating cost in the scheduling period is calculated as 926.715$.

It can be seen from Fig. 8 that:

1) Based on known parameters, MT1 has large output power, low start-stop cost and fuel cost, and high generation efficiency. It is thus mainly used to undertake basic load and remains operational in the 24 h period.

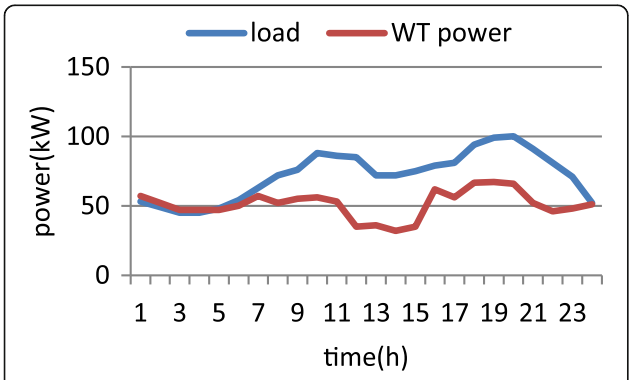

Fig. 6 Load and wind power forecasting curve

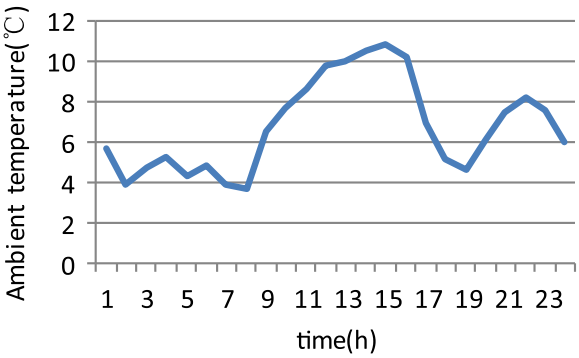

Fig. 7 Ambient temperature forecasting curve

2) It is known from Table 1 that MT2 has small output power, high start-stop cost and fuel cost, and low generation efficiency. It is thus used as a reserve set and is off during the whole studying period.

3) In the study, renewable energy power generation (e.g. WT) is used first. The use of temperature controlling devices increases renewable energy consumption without wind curtailment.

4) The lead-acid battery is charged from 3:00–7:00 when there's low load and discharged from 20:00–22:00 when the load is high.

5) Service life of the lead-acid batter is closely related to the depth of charge and discharge. Figure 8 shows that the energy storage system charges and discharges frequently in the coming 24 h, indicating a significant loss of energy storage system life.

② Optimal economic operation of the microgrid with temperature adjustment

Incorporated temperature controlling devices (e.g. heat pump) need adequately participate in demand response. At the same time, the allowed temperature adjustment range is set at ±2 °C and the load curve in the scheduling period is optimized considering user comfort. The optimal power generation scheduling of the microgrid with temperature adjustment is presented in Fig. 9. The total system operating cost in the scheduling period is 846.701$.

From Fig. 9, it can be seen that:

1) MT1 is mainly used to undertake basic load and keeps running in the scheduling period. However, the overall output decreases and becomes more stable in the scheduling period compared to that without temperature adjustment.
2) Similar to previous case, MT2 is used as a reserve set and remains off during the studying period.
3) Renewable energy power generation (e.g. WT) is used first. The use of temperature controlling

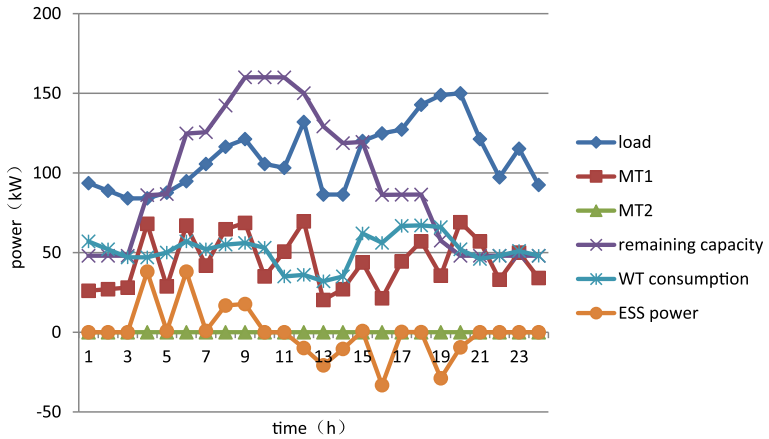

Fig. 8 Optimal power generation scheduling of microgrid without temperature adjustmen

devices increases renewable energy consumption, and wind energy can be fully absorbed in the microgrid.

4) The lead-acid battery is charged from 3:00–5:00 during low load and discharged from 19:00–23:00 during high load.
5) Time series load in the coming 24 h is optimized according to the temperature control characteristics, leading to few charges and discharges, small power and depth of charge–discharge of the energy storage system.

Comparing Figs. 8 and 9, the case with temperature adjustment of temperature controlling devices achieves 8.63% lower system operating cost than that without temperature adjustment. Moreover, the charge–discharge cycles of lead-acid battery decrease from 10 to 7 when temperature adjustment is enabled and the depth of charge–discharge also decreases, leading to increased service life of the energy storage system.

③ Effect of the allowed temperature adjustment range on operating cost

The operating costs of the microgrid without and with different temperature adjustment ranges (±1 °C ~ ±4 °C) are analyzed. During the study, other parameters are fixed and the results are shown in Fig. 10.

It can be known from Fig. 10 that increasing the allowed temperature adjustment range of the temperature controlling devices gradually decreases the operating costs in the scheduling period.This indicates that reasonable scheduling of temperature controlling devices can improve the economic efficiency of the microgrid.

④ Analysis of adjusted temperature of the temperature controlling devices

Adjusting the temperature of the temperature controlling devices can not only indirectly control the loads of the community microgrid, but also satisfy the comfort of residential users. The comparison between ambient

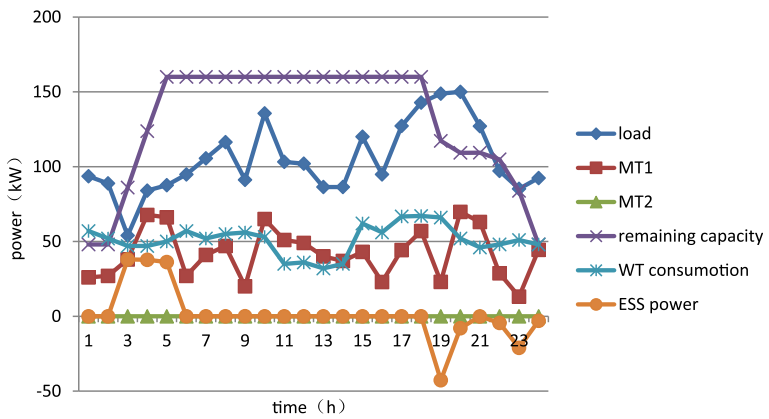

Fig. 9 Optimal power generation scheduling of microgrid with temperature adjustment

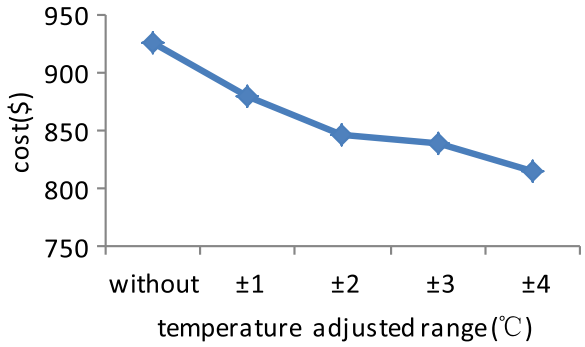

Fig. 10 Influence of Temperature adjustment ranges on the economy of microgrid

temperature and adjusted temperature without temperature adjustment is shown in Fig. 11. With temperature adjustment, the temperature controlling devices will switch between on and off when the adjusted temperature exceeds the limits, making the adjusted temperature change in up-down-up manner. Comparison of the ambient and adjusted temperatures with temperature adjustment is shown in Fig. 12.

It can be observed from Fig. 11 that without temperature adjustment, the adjusted temperature increases continuously until reaching the peak and then becomes stable. The average adjusted indoor temperature in the coming 24 h reaches as high as 32.4 °C which well exceeds the comfort of residential users. In contrast, Fig. 12 shows that with temperature adjustment, the indoor temperature is within users' comfort level, averaging at 24.4 °C.

7 Conclusions

This paper optimizes the time series output of temperature controlling devices through temperature adjustment by combining the dynamic variation law of adjusted temperature and power consumption, thus indirectly adjusting power load. An optimal economic operation model of microgrid is established, which takes the minimum sum of fuel cost, start-stop cost, penalty for wind curtailment and cost of energy storage loss as the objective function. The model is solved by HPSO algorithm which is easy-to-operate, has high accuracy, and overcomes local optimum. An isolated community microgrid with heat pump is used in the case study and the heat pump properly participates in microgrid scheduling according to the temperature adjustment characteristics. The results show that temperature adjustment of temperature controlling devices can not only improve the economic efficiency of the microgrid, but also reduce charge–discharge cycles of the energy storage system and increase microgrid schedulability. In practical engineering applications, temperature controlling devices can adopt more complicated control strategies and realize minute-based scheduling of the microgrid which will be the key content of our future research.

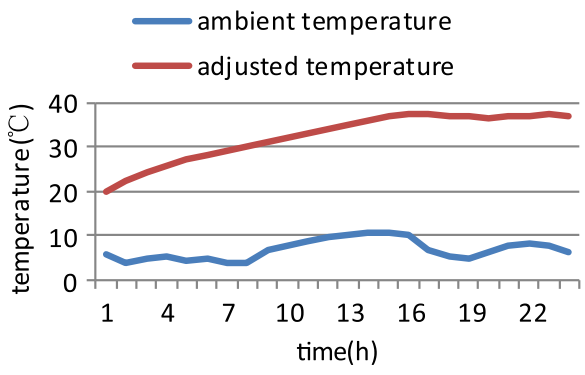

Fig. 11 The comparison of ambient temperature and adjusted temperature without temperature adjustment

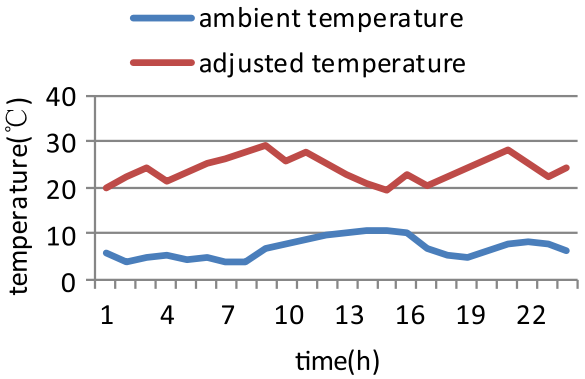

Fig. 12 The comparison of ambient temperature and adjusted temperature with temperature adjustment

Acknowledgements
This work was supported in part by the National Natural Science Foundation of China under Grant 51677011.

Authors' contributions
BH carried out the model of the optimal economic of community microgrid incorporating temperature controlling devices and participated in the design of the study. HW participated in the design of the study, statistical analysis and drafting the manuscript. SY participated in the design of the study, statistical analysis. All authors read and approved the final manuscript.

Competing interests
The authors declare that they have no competing interests.

Received: 24 August 2016 Accepted: 7 February 2017
Published online: 10 March 2017

Reference

1. Lu, Z., Wang, C., Mim, Y., Zhou, S., Lv, J., & Wang, Y. (2007). On the Research of Microgrid[J]. *Automation of Electric Power Systems, 31*(19), 100–107.
2. ISC Committee. (2003). *IEEE standard for interconnecting distributed resources with electric power systems[J]*. New York: Institute of Electrical and Electronics Engineers.
3. Lasseter R, Akhil A, Marnay C, et al. The CERTS microgrid concept[J]. White paper for Transmission Reliability Program, Office of Power Technologies, US Department of Energy, 2002, 2(3):30. http://pserc.wisc.edu/documents/

research_documents/certs_documents/certs_publications/certs_microgrid/certsmicrogridwhitepaper.pdf
4. Lasseter R H, Paigi P. Microgrid: a conceptual solution[C]//Power Electronics Specialists Conference, 2004. PESC 04. 2004 IEEE 35th Annual. IEEE, 2004, 6: 4285–4290
5. Su, L., Zhang, J., Wang, L., Miao, W., & Wu, Z. (2010). Study on some key problems and technique related to microgrid [J]. *Power System Protection and Control, 38*(19), 235–239.
6. Jin, P., Ai, X., & Xu, J. (2012). An Economic Operation Model for Isolated Microgrid Based on Sequence Operation Theory [J]. *Proceedings of the CSEE, 32*(25), 52–59.
7. Xu Lizhong, Yang Guangya, Xu. Zhao, E. Al. Combined scheduling of electricity and heat in a microgrid with volatile wind power[J]. Automation of Electric Power Systems, 2011, 35(9): 53–60
8. Niknam, T., Meymand, H. Z., & Mojarrad, H. D. (2011). A practical multi-objective PSO algorithm for optimal operation management of distribution network with regard to fuel cell power plants[J]. *Renewable Energy, 36*(5), 1529–1544.
9. Shen, Y., Hu, B., Xie, K., Xiang, B., & Wan, L. (2014). Optimal Economic Operation of Isolated Microgrid Considering Battery Life Loss [J]. *Power System Technology, 38*(09), 2371–2378.
10. Li, Z., Zhang, F., Liang, J., Yun, Z., & Zhang, J. (2015). Optimization on Microgrid With Combined Heat and Power System [J]. *Proceedings of the CSEE, 35*(14), 3569–3576.
11. Chen, J., Yang, X., Zhu, L., Zhang, M., & Li, Z. (2013). Microgrid Multi-objective Economic Dispatch Optimization [J]. *Proceedings of the CSEE, 33*(19), 57–66.
12. Peng, C., Xie, P., Zhan, J., & Sun, H. (2014). Robust Economic Dispatch of Microgrid Using Improved Bacterial Foraging Algorithm [J]. *Power System Technology, 38*(09), 2392–2398.
13. Wu, X., Wang, X., Wang, J., & Bie, Z. (2013). Economic Generation Scheduling of a Microgrid using Mixed integer programming [J]. *Proceedings of the CSEE, 33*(28), 1–9.
14. Wang, R., Gu, W., & Wu, Z. (2011). Economic and Optimal Operation of a Combined Heat and Power Microgrid with Renewable Energy Resources[J]. *Automation of Electric Power Systems, 35*(08), 22–27.
15. Gu, W., Wu, Z., Bo, R., et al. (2014). Modeling, planning and optimal energy management of combined cooling, heating and power microgrid: A review[J]. *International Journal of Electrical Power & Energy Systems, 54*(1), 26–37.
16. Wu, X., Wang, X., Bie, Z., & Wang, J. (2013). Economic operation of microgrid with combined heat and power system[J]. *Electric Power Automation Equipment, 33*(08), 1–6.
17. Zhang, J., Cheng, H., Hu, Z., Ma, Z., Zhang, J., & Yao, L. (2009). Power System Probabilistic Production Simulation Including Wind Farms [J]. *Proceedings of the CSEE, 29*(28), 34–39.
18. Guo, Y., Hu, B., Wan, L., Xie, K., Yang, H., & Shen, Y. (2015). Short-term Economic Scheduling of CHP Microgrid Incorporating Heat Pump [J]. *Automation of Electric Power Systems, 39*(14), 16–22.
19. Callaway, D. S., & Hiskens, I. A. (2011). Achieving controllability of electric loads[J]. *Proceedings of the IEEE, 99*(1), 184–199.
20. Katipamula S, L. N. Evaluation of residential HVAC control strategies for demand response programs[J]. Transactions-american society of heating refrigerating and air conditioning engineers, 2006, 112(1): 535.
21. Lu, N. (2012). An evaluation of the HVAC load potential for providing load balancing service[J]. *IEEE Transactions On Smart Grid, 3*(3), 1263–1270.
22. Kou, B., Yang, T., Zhang, X., Zhang, Q., Liu, W., & Ge, J. (2007). A New Hybrid Particle Swarm Optimization Based on Crossover and Mutation [J. *Computer Engineering and Applications, 43*(17), 85–88.